On the appearance of multiple attractors in discrete food-chains

Danny Fundinger
Laboratory of Mathematical Modelling,
Department of Mathematics
Sankt Petersburg State Polytechnic University
Sankt Petersburg, 195251, RUSSIA
e-mail research@danny.fundinger.de

Torsten Lindström
Department of Chemistry and Biomedical Science,
University of Kalmar
S-39182 KALMAR, SWEDEN
e-mail torsten.lindstrom@hik.se

George Osipenko
Laboratory of Mathematical Modelling,
Department of Mathematics
Sankt Petersburg State Polytechnic University,
Sankt Petersburg, 195251, RUSSIA
e-mail george.osipenko@mail.ru

Abstract

Klebanoff and Hastings (1994) detected cases of multiple attractors in continuous food-chains. In this paper we discuss similar phenomena in the discrete food-chains introduced by Lindström (2002). The results imply that the dynamical properties including species persistence may change due to disturbances that do not involve changes in the environmental parameters. Thus, there are possibilities that species may be eradicated or start to oscillate at different frequencies without any changes in the environment. Since this is now shown to hold in both seasonal and non-seasonal environments, we expect that this is a rather general property of ecosystems.

Keywords: discrete food-chain, multiple attractors, orientability
AMS subject classification: 92D40, 37M05, 65P99

1 Introduction

Lindström (2002) proposed a model for discrete food-chains that displays a lot of properties commonly known for continuous food-chains (Rosenzweig (1973), Gragnani, DeFeo, and Rinaldi (1998)). Klebanoff and Hastings (1994) and later Kuznetsov, DeFeo, and Rinadi (2001) pointed out that multiple attractors may be involved in such continuous food-chains. It was reported in Lindström (2002) and Gyllenberg, Hanski, and Lindström (1996) that multiple attractors normally exist already in discrete predator-prey systems.

In this paper we analyze a number of more delicate ways how multiple attractors (invariant sets possessing asymptotic stability by Lyapunov) may evolve in three-dimensional ecosystems. Neimark-Sacker bifurcations describe to a large extent the transistions from stable to unstable behavior in discrete food-chains. After a Neimark-Sacker bifurcation an invariant non-smooth circle usually appears (Kutsnetsov (1998)) and the dynamics on the invariant circle can shortly after the Neimark-Sacker bifurcation be understood as a circle map (Wiggins(2003)). The dynamics of circle maps usually contains resonance tongues describing structurally stable periodic behavior and structurally unstable quasi-periodic behavior. As we proceed further away from the Neimark-Sacker bifurcation, the circle map description breaks down and the resonance tongues start merging. At paramater values corresponding to merging resonance tongues, multiple attractors can normally be detected (Aronson, Chory, Hall, and McGehee (1982) and Gyllenberg, Hanski, and, Lindström (1996)). The descriptions of these phenomena has so far been restricted to phenomena in 2-dimensional state spaces and we now do attempts to describe these phenomena in 3-dimensional state space. We give examples on how certain bifurcation sequences can be connected to disappearance of orientation of certain invariant manifolds. These are phenomena that cannot be analyzed completely in 2-dimensions. We proceed with an analysis of the reported mathematical phenomena and link this to possible consequences for population dynamics.

A number of advanced numerical methods is needed for the analysis of the model in Lindström (2002). One of these methods is the construction of the symbolic image graph (Osipenko (1983,2004), Avrutin, Fundinger, Levi, Osipenko, and Schanz (2006) and Fundinger (2005)) in order to compute an outer covering of the chain-recurrent set, see (Devaney (1989) and Guckenheimer and Holmes (1983)). By application of this method, return trajectories of any type can be localized. In our context, the technique was successfully applied to provide information of otherwise invisible unstable quasiperiodic oscillations. For the computation of periodic cycles, we applied the RIM method (Fundinger (2006)). This method is an alternative to the standard approach of using a Newton-based iteration scheme which has the advantage that neither an initial guess is required nor the computation of any Jacobian-like matrix. We applied the RIM method for computation of both, stable and unstable periodic orbits. The method proved useful for localization of coexisting attractors, too. By minor modifications (cf. Fundinger (2006)), the RIM method can also be applied to approximate parts of the stable manifolds. Additionally, we used some stan-

dard techniques for analysis, like computation of forward iterates and dominant Lyapunov exponents. All of the above mentioned techniques are implemented as part of the non-commercial AnT software package (cf. Avrutin, Lammert, Schanz, Wackenhut, and Osipenko (2003)) (see (AnT (2005)) for download). Most of our computations were carried out with this tool. The only applied technique not included in the AnT package, was the iteration of a specific chosen curve. If appropriate starting points are given, this method allows an approximation of the form of an invariant manifold which is completely specified by the starting points given. It connects the iterates of the starting points and extracts information about the dynamics on the manifold. The method is still under development.

The paper is organized as follows. We start by formulating the model and compute its equilibria. Then we give an overview about the main dynamical characteristics of the system. We start from a parameter setting at which the computation and analysis of system features are comparatively easy. Afterwards, we describe the area of investigation in parameter space where coexisting attractors can be found. The occurrence of these multiple attractors is the subject of the following chapter. We list several examples leading to initial value dependent dynamical patterns and discuss under what circumstances such behavior may evolve in our system and what potential reasons may create such behavior in general ecological systems.

2 The model and its equilibria

We define the model under study here by the discrete dynamical system

$$\begin{aligned} X_{t+1} &= \frac{M_0 X_t \exp(-U_t)}{1 + X_t H(\exp(-Z_t), \frac{U_t}{1-\exp(-Z_t)})}, \\ U_{t+1} &= M_1 X_t U_t \exp(-Z_t) K(U_t) \cdot K(M_2 U_t Z_t), \\ Z_{t+1} &= M_2 U_t Z_t. \end{aligned} \tag{1}$$

The two special functions referred to above are given by

$$H(\alpha, \rho) = -\exp(-\rho)(\mathrm{Ei}(\rho) - \mathrm{Ei}(\alpha\rho)) \log \alpha \tag{2}$$

and

$$K(\gamma) = \begin{cases} \frac{1-\exp(-\gamma)}{\gamma}, & \text{if} \quad \gamma \neq 0. \\ 1, & \text{if} \quad \gamma = 0 \end{cases}, \tag{3}$$

The model was derived in Lindström (2002), with an explanation of all involved parameters and variables. The variables are related to the different trophic levels of the system, so X is proportional to the vegetation abundance whereas Z is proportional to the carnivore abundance. Since the relation between herbivores and U is nonlinear, a more complicated relation describes the situation

here. However, such relationships do not change the topological properties of the system under study. So, for convenience, we will refer to the vegetation, herbivore, and carnivore levels in the sequel.

The above model contains exponential integrals. Well-working approximations are therefore needed especially for theoretical studies of the model. An approximation already introduced by Lindström (2002) can be defined by

$$\begin{aligned} X_{t+1} &= \frac{M_0 X_t \exp(-U_t)}{1 + X_t \max(\exp(-U_t), K(Z_T)K(U_t))} \\ U_{t+1} &= M_1 X_t U_t \exp(-Z_t) K(U_t) \cdot K(M_3 U_t Z_t) \\ Z_{t+1} &= M_2 U_t Z_t. \end{aligned} \tag{4}$$

This approximation seems to work well not only in theoretical computations. The original model (1) contains numerical difficulties that are removed in the approximation (4), cf Lindström (2002). Note that in the original equation $M_2 = M_3$. The fourth parameter M_3 is introduced in order to generate additional cases allowing an analysis as complete as possible of the system characteristics (see Sec. 3). We have not made any attempts to clarify the biological relevance of this parameter. Note that the solutions of (4) remain positive and bounded (repeating the arguments in Lindström (2002) shows that all solutions starting in the positive cone enter the box $0 < X_t < M_0$, $0 < U_t < M_0 M_1$, $0 < Z_t < M_0 M_1 M_2^2 / M_3$ within three iterations).

The system (4) has at most four equilibria and they are given by:

$$\begin{aligned} E_0 &= (0, 0, 0) \\ E_1 &= (M_0 - 1, 0, 0) \\ E_2(X_*, U_*, Z_*) &= \left(\frac{M_0 \log\left(\frac{M_1 M_0}{1+M_1}\right)}{(M_0 - 1)M_1 - 1}, \log\left(\frac{M_1 M_0}{1 + M_1}\right), 0 \right) \end{aligned} \tag{5}$$

and that a fourth is given by

$$\begin{aligned} E_4(\tilde{X}, \tilde{U}, \tilde{Z}) \quad = \quad & \\ & \left(\frac{M_0 \exp(-\frac{1}{M_2}) - 1}{K\left(\frac{1}{M_2}\right) K\left(\log M_1 \left(M_0 \exp(-\frac{1}{M_2}) - 1\right)\right)}, \right. \\ & \left. \frac{1}{M_2}, \log M_1 \left(M_0 \exp(-\frac{1}{M_2}) - 1\right) \right) \end{aligned}$$

if $M_2 = M_3$ and

$$\max(\exp(-\tilde{U}), K(\tilde{U})K(\tilde{Z})) \quad = \quad K(\tilde{U})K(\tilde{Z}). \tag{6}$$

Uniqueness of the last equilibrium follows from the fact that the right hand-side of

$$1 = M_1 \frac{M_0 \exp(-1/M_2) - 1}{\max\left(\exp(-\frac{1}{M_2}, K(\frac{1}{M_2})K(Z))\right)} K(\frac{1}{M_2}) \exp(-Z) K(\frac{M_3}{M_2} Z)$$

is a continuous and strictly decreasing function of Z. In order to see this, consider the derivative of the function $\exp(-Z)K(aZ)/K(Z)$, for $Z > 0$ and $\alpha > 0$. This derivative equals a positive function times

$$a\exp(Z) - a + \exp(Z) - \exp((a+1)Z).$$

Use of the usual Maclaurin expansion for $\exp(Z)$ shows now that the expression above is negative. Thus, at most four equilibria exist for system (4) in the non-negative octant.

3 Two attractors on the Möbius strip

In order to study the main characteristics and structure of the coexisting attractors, we commence by analyzing the system (4) at the parameter position $M_0 = 4.0$, $M_1 = 1.0$, $M_2 = 3.0$, $M_3 = 4.0$. At this parameter position all invariant curves turn out to be low-periodic orbits, which is a good starting point for a rigorous analysis of important basic asymptotic features of the system. Later, we shall modify parameters in order to achieve values that we know have biological relevance ($M_2 = M_3$) and follow up with a discussion of what bifurcation sequences may yield multiple attractors in biological food-chain systems.

The above parameter setting yields two attractors. These attractors are 16-periodic cycles. Additionally, we can find the 4 fixed points alluded to above, and three further periodic cycles, namely a 16-periodic and two 8-periodic ones. The RIM method provides an efficient tool for computing these orbits, see Fundinger (2006).

The two 16-periodic cycles, which are the attractors of the system, can be generated by initial data according to

$$S_1^{16} \approx \left\{ \begin{pmatrix} 2.7540 \\ 0.2977 \\ 0.02869 \end{pmatrix}, \dots \right\}, S_2^{16} \approx \left\{ \begin{pmatrix} 0.9889 \\ 0.9753 \\ 0.1610 \end{pmatrix}, \dots \right\} .$$

A computation of the eigenvalues along these cycles confirms that

$$e_1(S_1^{16}) \approx 0.0087, \quad |e_{2,3}(S_1^{16})| \approx |0.9161 \pm 0.1832i| = .9342 \quad < 1, \qquad (7)$$
$$e_1(S_2^{16}) \approx 0.0079, \quad |e_{2,3}(S_2^{16})| \approx |0.8672 \pm 0.2166i| = .8938 \quad < 1, \qquad (8)$$

which shows that the eigenvalues of both cycles are located inside the complex unit circle. Consequently, these cycles are attracting periodic orbits.

Now we proceed by giving the unstable periodic orbits. One of them is 16-periodic and can be generated by:

$$U_1^{16} \approx \left\{ \begin{pmatrix} 0.9109 \\ 0.4561 \\ 0.4268 \end{pmatrix}, \dots \right\} ,$$

whereas two are 8-periodic,

$$U_1^8 \approx \left\{ \begin{pmatrix} 1.8548 \\ 1.1184 \\ 0.4369 \end{pmatrix}, \dots \right\}, U_2^8 \approx \left\{ \begin{pmatrix} 2.2910 \\ 0.0807 \\ 0.2726 \end{pmatrix}, \dots \right\} .$$

The eigenvalues for the unstable cycles are given by:

$$e_1(U_1^{16}) \approx 0.0105, \qquad e_2(U_1^{16}) \approx 1.0874, \qquad e_3(U_1^{16}) \approx 0.6492, \tag{9}$$

$$e_1(U_1^{8}) \approx 1.0988, \qquad e_2(U_1^{8}) \approx -0.1084, \qquad e_3(U_1^{8}) \approx -0.7945 \tag{10}$$

$$e_1(U_2^{8}) \approx -1.1252, \qquad e_2(U_2^{8}) \approx 0.8983, \qquad e_3(U_2^{8}) \approx -0.0800 \tag{11}$$

For each of these cycles, one eigenvalue lies outside the unit circle, and two are inside. Thus, the cycles are of saddle type. The stable manifolds of these saddles are 2-dimensional, the unstable ones are 1-dimensional.

Considering the properties of the periodic cycles, we can conclude that they belong to a one-dimensional invariant manifold $\mathcal{M}$. This manifold consists of the periodic cycles and the unstable manifolds of the saddles so that

$$\mathcal{M} = S_1^{16} \cup S_2^{16} \cup U_1^{16} \cup U_1^8 \cup U_2^8 \cup W^u(U_1^{16}) \cup W^u(U_1^8) \cup W^u(U_2^8).$$

In order to approximate $\mathcal{M}$, we computed the unstable manifolds of the saddles. This is done by the computation of several forward iterates starting in the vicinity of the saddle points. The numerical approximation of $\mathcal{M}$ is shown in Fig. 1(a), whereby the periodic cycles and the unstable manifolds of the saddles are colored differently. Obviously, $\mathcal{M}$ consists of eight similar parts in the phase space. Each of these parts corresponds to a set of saddles and period-two sinks of the map f^8, which is denoted as the eighth iterated of the system function f as defined by Eq. 4. The enlargement of one of these parts, as illustrated in Fig. 1(b), clarifies the structure of the system. The unstable manifolds of the 8-periodic cycle U_2^8 leads to S_1^{16} and the unstable manifold $W^u(U_1^{16})$ leads to S_1^{16} and S_2^{16}.

Next we outline the relation between the two saddles U_1^8 and U_2^8. Therefore we computed parts of the stable manifold of U_2^8, i.e. $W^s(U_2^8)$. Note that, due to the complexity of the underlying system, the computation of the stable manifold is a nontrivial task. Indeed, we are only able to compute a rough approximation of the local stable manifold in the vicinity of U_2^8. We applied the RIM method as described in Fundinger (2006) and computed an outer covering of those parts of the stable manifolds for which forward iterates come close to the saddle within 100 iteration steps. As can be seen in Fig. 2, the unstable manifold $W^u(U_1^8)$ intersects with $W^s(U_2^8)$ so that $W^u(U_1^8)$ oscillates around $W^s(U_2^8)$. Thus, our numerical results indicate that the unstable manifold $W^u(U_1^8)$ intersects the stable manifold of U_2^8 transversally on the Möbius strip, and therefore the heteroclinic structure found here is a structurally stable phenomenon, cf Guckenheimer and Holmes (1983) and Kuznetsov (1994).

Due to the fact that all minimal attractors (i.e. attractors that do not contain other attractors) of the system belong to $\mathcal{M}$, there is a minimal two

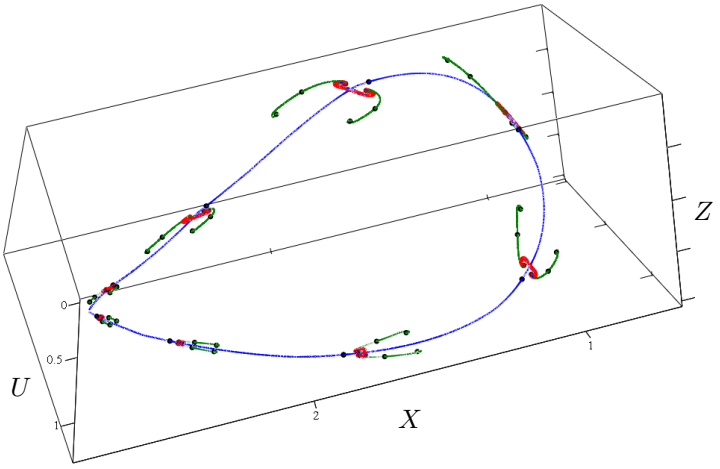

(a)

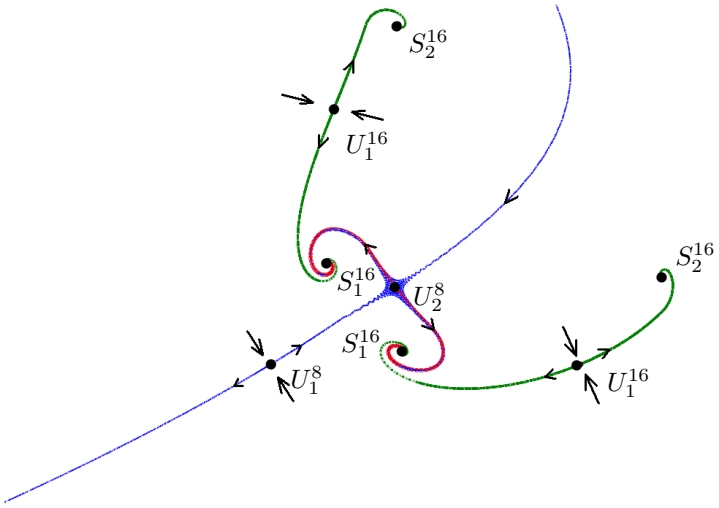

(b)

Figure 1: *(a): Numerical approximation of the invariant manifold $\mathcal{M}$ of the 8- and 16-periodic cycles for $M_0 = 4.0$, $M_1 = 1.0$, $M_2 = 3.0$, $M_3 = 4.0$ and the unstable manifolds of U_1^8 (blue), U_2^8 (red) and U_1^{16} (dark green). (b): Enlargement of one of the eight similar parts of $\mathcal{M}$. Arrows indicate the direction of the flow.*

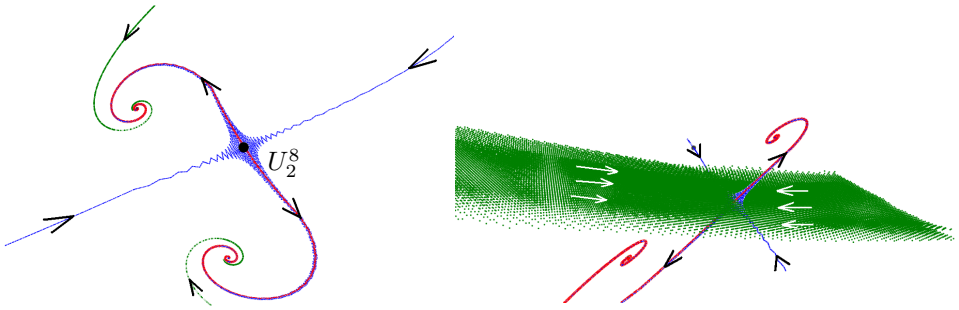

(a) (b)

Figure 2: *(a):The unstable manifold of U_1^8 (blue) in the vicinity of U_2^8. (b): Numerical approximation of parts of the stable manifold of U_2^8 (dark green). White and black arrows indicate the direction of the flow.*

dimensional invariant manifold $\mathcal{M}_2$ which contains $\mathcal{M}$ and is Lyapunov stable. Such a manifold can be approximated using iterates of specific curves, cf Section 1.

The results of a computation are shown in Fig. 3(a). It is clear that $\mathcal{M}_2$, as $\mathcal{M}$, consists of eight similar parts. Each of the eight similar parts is mapped to its neighbor so that after eight iterates it is mapped into itself. Thus, the manifold $\mathcal{M}_2 = \bigcup V_i,\ i = 1, 2, ..., 8$ consists of eight homeomorphic pieces. One of them is illustrated in Fig. 3(b).

The manifold $\mathcal{M}_2$ turns out to be homeomorphic to a Möbius strip. More precisely, consider the restriction of the dynamical system to $\mathcal{M}_2$ and the eigenvectors EV_1, EV_2, EV_3 corresponding to the eigenvalues $e_1(U_2^8)$, $e_2(U_2^8)$, $e_3(U_2^8)$, see Eq. 11. Let A be a point located at the periodic orbit U_2^8 and denote the system function defined by Eq. 4 as f. The invariant subspace spanned by EV_1 and EV_2 (or EV_3) is a tangent space $T\mathcal{M}_2(A)$ to $\mathcal{M}_2$ at the point A. The differential $Df^8(A)$ restricted to $T\mathcal{M}_2(A)$ changes orientation because the first eigenvalue $e_1(U_2^8) > 1$ and $e_2(U_2^8) < 0$ (or $e_3(U_2^8) < 0$), i.e.

$$\det(Df^8(A))|_{T\mathcal{M}_2(A)} = e_1(U_2^8)\, e_2(U_2^8) < 0.$$

At the same time, from continuity it follows that the map $f : V_i \to V_{i+1}$ saves orientation. This is possible only if the manifold $\mathcal{M}_2$ is non-orientable. The manifold $\mathcal{M}_2$ is two-dimensional and thus, it must be a Möbius strip.

As already mentioned, the unstable manifold of the 8-periodic hyperbolic orbit U_2^8 ends at the 16-periodic sink S_1^{16}. Thus, considering the map f^8, $W^u(A)$ ends at a two-periodic sink $P^2 = \{P_1, P_2\} \subset S_1^{16}$. Hereby, the map f^8 changes orientation and maps P_1 to P_2.

Taking the geometrical point of view, we could say that the 8-periodic cycles

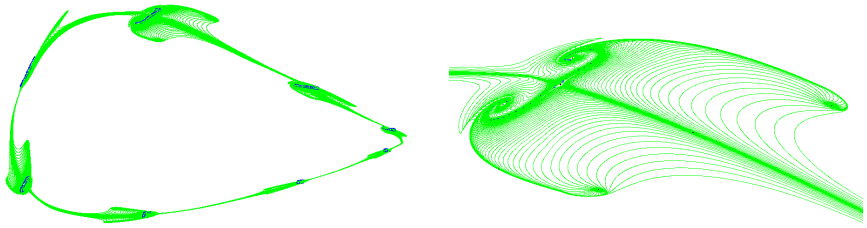

(a) (b)

Figure 3: *(a) Numerical approximation of the two dimensional invariant manifold $\mathcal{M}_2$ for $M_0 = 4.0$, $M_2 = 3.0$, $M_3 = 4.0$ by curve iteration. (b) One of the eight homeomorphic parts $V_i \subset \mathcal{M}_2, i = 1, 2, \ldots, 8$.*

U_1^8 and U_2^8 lie on the center line of the Möbius strip, and the 16-periodic cycles S_1^{16}, S_2^{16} and U_1^{16} on its outer boundary.

Some general characteristics regarding the occurrence of multiple attractors can already be identified. Firstly, if multiple attractors exist, they are situated close to each other in the phase space. The attractors are invariant cycles, either periodic or quasi-periodic. Geometrically, each of them forms the boundary of a Möbius strip and there is an invariant curve of saddle type, also on the boundary of a Möbius strip, in between these attractors. These characteristics fit to all multiple attractors that we were able to localize.

4 Scenario of bifurcations

Our numerical studies confirm that the system dynamics are governed by just one attractor in large parts of the parameter space. Thus, we detected coexisting attractors only in a small range of the parameter space. Consequently, we limit the rest of the discussion to the parameter range $M_0 \in [3.3; 3.6]$ and fix the other parameters to $M_1 = 1.0, M_2 = M_3 = 4.0$. So far, multiple attractors seem to be located in the vicinity of this slot. We commence an overview about some general features and bifurcations before we proceed in the next section with a detailed analysis for selected parameter values possessing multiple attractors.

The selected area is located along the route to chaos. At $M_0 \approx 2.93$ a Neimark-Sacker bifurcation occurs. The fixed point E_4 loses its stability and an invariant curve is born, see Fig. 4. This curve becomes the minimal attractor of the system. We denote it by $\mathcal{A}$. As the parameter M_0 is increased, the attractor $\mathcal{A}$ is alternatingly quasi-periodic and periodic, like the dynamics of circle maps (Devaney (1989) and Wiggins (2003)). This holds as long as the parameter

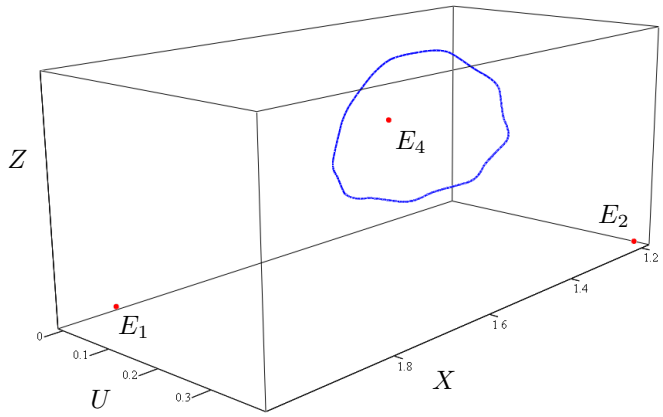

Figure 4: *Numerical computation of the minimal attractor $\mathcal{A}$ (blue) and the fixed points E_1, E_2, E_4 at $M_0 = 2.935$, shortly after a Neimark-Sacker bifurcation.*

value stays moderately far from the bifurcation value, cf Aronson, Chory, Hall, and McGehee (1982).

Some general features of the selected area can be described by dominant Lyaponov exponents, see Figure 5. We used the implementation (AnT (2005)) of the algorithm described in Wolf, Swift, Swinney, Vastano (1985) for this computation. The general patterns described by alternating periodic and quasiperiodic motion alluded to above is confirmed in the Figure, negative values indicate that at least one periodic attractor exists, values around zero indicate quasi-periodic motion, or otherwise structurally unstable cases. Positive values indicate at least one chaotic attractor. If several attractors exist, the dominant Lyapunov exponent corresponding to the attractor having $(X, U, Z)^T = (0.927, 0.527, 0.112)^T$ in its basin of attraction was computed. Our objective was actually a plot of the different Lyapunov exponents of different attractors in the same diagram in order to be able to visualize sharply the regions possessing initial value dependent dynamics. However, for cases when multiple attractors were detected in this study, their Lyapunov exponents turned out to follow each other too close in magnitude for this to make sense (cf. (7) and (8)).

We next analyze the structure of the attractor in the selected area by choice of a particular parameter value. We choose $M_0 = 3.4001$ and construct an outer covering of the chain recurrent set (cf. Guckenheimer and Holmes (1983)) by means of the symbolic image method, see Osipenko (1983), Osipenko (2004), and Fundinger (2005).

The results are displayed in Figure 6. Four unstable fixed points are located together with two invariant curves, one of them is unstable and the other one turns out to be the minimal attractor, $\mathcal{A}$, of the system. The unstable invari-

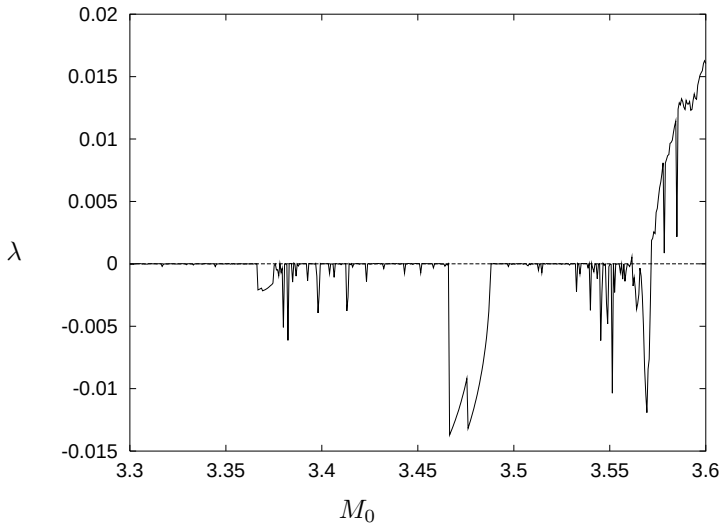

Figure 5: *Plot of the largest Lyapunov exponents* λ *of the minimal attractor* $\mathcal{A}$ *in the parameter range* $M_0 \in [3.3; 3.6]$.

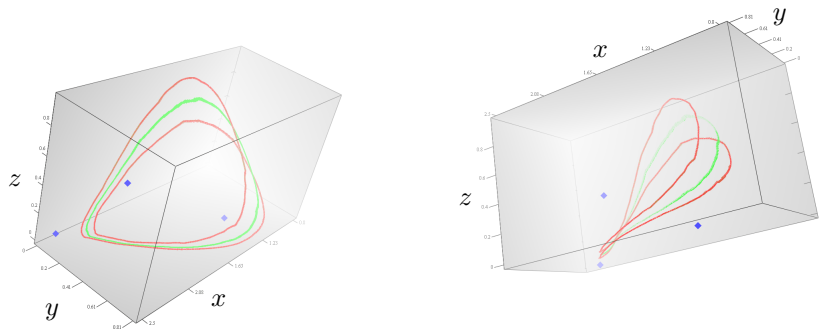

(a) (b)

Figure 6: *Two different views of the outer covering of the chain recurrent set at position* $M_0 = 3.4001$. *The attractor* $\mathcal{A}$ *(red), an unstable invariant curve (green) and the unstable fixed points (blue) are shown. The fourth fixed point at* $(0, 0)$ *is not visible here.*

ant curve was born at the Neimark-Sacker bifurcation at $M_0 \approx 2.93$ and looses its stability at $M_0 \approx 3.366$. At this position a bifurcation happens and a new stable invariant cycle is born. The bifurcation reminds about the type of period doubling bifurcation that is usually observed in continuous dynamical systems. However, we can not speak of period doubling bifurcations here in the same sense as is usually meant for discrete systems. We rather observe a pattern that is typical for continuous systems (cf. Feigenbaum (1978,1980) Guckenheimer and Holmes (1983)) in a discrete system. The emerged cycle becomes the minimal attractor $\mathcal{A}$ of the system and both cycles are illustrated in Fig. 6. These two cycles belong to a two dimensional invariant manifold $\mathcal{M}_2$ which is homeomorphic to our old friend, the Möbius strip, cf Section 3.

Geometrically, the curves resemble the shape of a Möbius strip. The stable invariant curve can be imagined as the edges of the strip, and the unstable curve as its center line. Numerical studies of forward and backward iterates so far indicate that the curve at the center line is of saddle type. We have not yet established this property by means of measures like, for instance, Lyapunov exponents.

The dominating Lyapunov exponent of the attractor $\mathcal{A}$ turns out to be $\lambda = 6.4766 \cdot 10^{-6}$, which together with numerical error bounds indicates that $\mathcal{A}$ is quasi-periodic. Unfortunately, similar quantities cannot be computed for the unstable invariant curve by means of numerical methods currently available to us. The sharpest answer was provided by the RIM method which confirmed a period higher than 64 in case it is periodic. Thus, we consider this as a quasi or high-periodic cycle. Since all quasi-periodic cases are structurally unstable, there are limits on how far we are able to pursue such a classification numerically.

The basic structure of the attractor remains as illustrated as long as no chaos is detected. Windows in parameter space can be observed for which the attractor is a periodic cycle. Later, we shall see that several more period doubling-like bifurcations of the same kind happen close to the transition to chaos. The stable invariant curve becomes unstable again, and a new stable invariant curve is born which winds around it. Hence, the attractor is on the edge of a Möbius strip which is embedded into another one and several more unstable invariant curves coexist.

5 Occurrence of multiple attractors

In this section we show the occurrence of multiple attractors within the parameter range discussed above. Our objective is to determine typical patterns of multiple attractors in our system. We focus on two windows in the parameter range. The first case involves two coexisting attractors which are invariant curves. The latter case involves periodic attractors only, which allows computation of the eigenvalues. We also show that a period-doubled Möbius strip appears between the two windows, and that the second scenario of multiple attractors happens close to the occurrence of chaos.

First we look at the interval $M_0 = [3.53195; 3.5332]$. Within this range

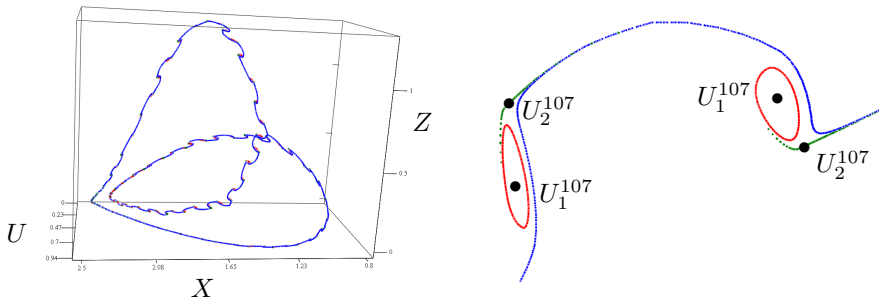

(a) (b)

Figure 7: *Numerical approximation of the two minimal attractors at* $M_0 = 3.532$. $\mathcal{A}_1$ *is quasi-periodic (blue) and* $\mathcal{A}_2$ *consists of* 107 *closed cycles (red) around a* 107*-periodic hyperbolic orbit* U_1^{107}. *Another* 107*-periodic orbit* U_2^{107} *is a saddle which separates the attractors. The unstable manifold of the saddle is also computed (dark green).*

several local and global bifurcations lead to a number of subsequent changes in the dynamics. This involves the appearance of two coexisting attractors after a saddle bifurcation, a boundary crisis between an attractor and a saddle, and the birth of a second coexisting attractor out of a periodic saddle. We proceed with the scenario that produces the coexisting attractors at the position $M_0 = 3.532$ and postpone a more detailed discussion of the bifurcation sequence to a subsequent paper.

The two attractors found are an invariant quasi-periodic curve, in the following denoted by $\mathcal{A}_1$, and an invariant set $\mathcal{A}_2$ which consists of 107 closed curves which are situated around an unstable 107-periodic orbit U_1^{107}. Hereby, $\mathcal{A}_2$ is an invariant quasi-periodic curve for the 107-th iterate of Eq. 4. In between $\mathcal{A}_1$ and $\mathcal{A}_2$, a 107-periodic saddle orbit U_2^{107} is situated. The two periodic orbits can be generated by

$$U_1^{107} \approx \left\{ \begin{pmatrix} 1.6284 \\ 0.1417 \\ 0.4878 \end{pmatrix}, \dots \right\}, U_2^{107} \approx \left\{ \begin{pmatrix} 1.6440 \\ 0.1369 \\ 0.4944 \end{pmatrix}, \dots \right\} .$$

The results of a computation are illustrated by Fig. 7. Hereby, $\mathcal{A}_2$ moves closer to U_1^{107} for an increase of M_0 (subcritical stable Neimark-Sacker). The radius of the cycles decreases and in $M_0 \approx 3.532833$ the stable cycles are absorbed by U_1^{107}. At this position, U_1^{107} becomes stable and is an attractor.

We also investigated the 2-dimensional stable manifold $W^s(U_2^{107})$ of the saddle U_2^{107}. We provide numerical evidence that the manifold separates the domains of attraction of $\mathcal{A}_1$ and $\mathcal{A}_2$ in Fig. 8(b). We first give a 1-dimensional

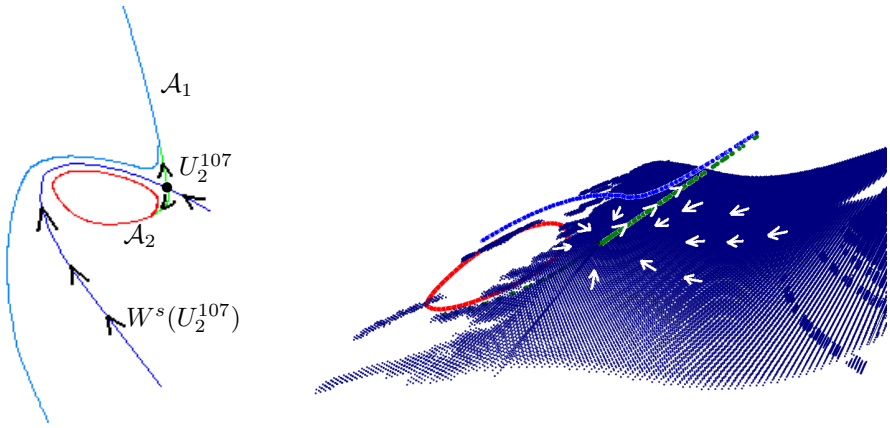

(a) (b)

Figure 8: *(a) Sketch of parts of the stable manifold of the saddle orbit* U_2^{107}*, i.e.* $W^s(U_2^{107})$*, which separates the attractors* $\mathcal{A}_1$ *and* $\mathcal{A}_2$*. The approximation shows a projection of the local stable manifold within the vicinity of one of the points belonging to* U_2^{107}*. Black arrows indicate the direction of the flow. (b) Numerical approximation of parts of the stable manifold* $W^s(U_2^{107})$ *(dark blue). The unstable manifold* $W^u(U_2^{107})$ *(green) and the attractors* $\mathcal{A}_1$ *(light blue) and* $\mathcal{A}_2$ *(red) are also shown. White arrows indicate the direction of the flow. The stable manifold* $W^s(U_2^{107})$ *separates the domains of attraction of* $\mathcal{A}_1$ *and* $\mathcal{A}_2$*.*

illustration of the manifold by numerical approximation computed by curve iterates in Figure 8(a). A 2-dimensional approximation is then shown in Fig. 8(b). This approximation was computed with the RIM method mentioned in Sec. 3 and produces an outer covering of those parts of the stable manifold for which the forward iterates come close to the saddle within 2500 iterations. Although only those parts of the stable manifold can be approximated which are situated in the vicinity of one point of the saddle orbit U_2^{107}, it is obvious that the stable manifold separates the domains of attraction. The structure of the complete stable manifold, as well as of the two domains of attraction it separates, is in general not only difficult to compute but also to visualize. Although we were able to compute larger parts of the stable manifolds as the one shown in Fig. 8(b), we were not able to give a meaningful interpretation regarding the position and size of the domains of attraction.

Let us next consider the eigenvalues of the periodic orbits which can be approximated as

$$|e_{1,2}(U_1^{107})| \approx |0.9950 \pm 0.2146i| \quad = 1.0179 > 1, \quad e_3(U_1^{107}) \approx 0, \tag{12}$$

$$e_1(U_2^{107}) \approx 1.3694, \quad e_2(U_2^{107}) \approx 0.6504, \quad e_3(U_2^{107}) \approx 0. \tag{13}$$

First of all, the eigenvalues confirm us the numerical results regarding U_2^{107} – the cycle is of saddle type and has a 1-dimensional unstable and a 2-dimensional stable manifold. Furthermore, the cycle U_1^{107} has a 1-dimensional stable and a 2-dimensional unstable manifold which spirals to the curves of $\mathcal{A}_2$. Note that each

of the periodic orbits has an eigenvalue close to 0. Due to the numerical error bounds a sharper answer is not possible. However, none of the eigenvalues is below or equal 0 because the determinant of the Jacobian, i.e. $\det(Df^{107}(U_{1,2}^{107}))$, is positive and, hence, $e_1e_2e_3 > 0$. We consider next the possibility of constructing a two-dimensional invariant manifold $\mathcal{M}_2$ which contains $\mathcal{A}_1$, $\mathcal{A}_2$, U_1^{107} and U_2^{107}. Due to the fact that $|e_{1,2}(U_1^{107})| > 1$, the eigenvector EV_3 corresponding to $e_3(U_1^{107})$ is transversal to $\mathcal{M}_2$. This confirms that $\mathcal{M}_2$ is Lyapunov stable.

We proceed with a bifurcation happening before occurrence of the next area in parameter space with multiple attractors. Close to $M_0 \approx 3.5331$ a period doubling-like bifurcation as described in Sec. 4 can be observed again. Our numerical evidence so far suggests that one attractor is located at the boundary of a Möbius strip that winds around the initial Möbius strip. We illustrate the situation by an invariant curve at position $M_0 = 3.5501$ in Fig. 9(a). The minimal attractor $\mathcal{A}$ at this position belongs to a two-dimensional invariant manifold $\mathcal{M}$ which is homeomorphic to the Möbius strip. However, there is also another two-dimensional invariant manifold $\mathcal{M}_2$ homeomorphic to a Möbius strip which contains $\mathcal{M}$ and also the invariant curve which was born after the Neimark-Sacker bifurcation at $M_0 \approx 2.93$. Note however, that we have not yet established this properties by measures. We give an illustration by computation of curve iterates at position $M_0 = 3.56$. The manifolds $\mathcal{M}$ and $\mathcal{M}_2$ can be approximated as shown in Fig. 9(b).

Next we present coexisting attractors which are all located on the boundary of a Möbius band which winds around another one. Therefore, we investigate the interval $M_0 \in [3.57; 3.5714]$. In this area, the actual transition to chaos appears and also multiple attractors can be observed. The area displays mainly a negative dominant Lyapunov exponent, cf Figure 5. Thus, at least one of the attractors must be periodic. Indeed, all attractors found here turned out to be periodic.

For a detailed study we choose the position $M_0 = 3.571$. Here, we find two coexisting attractors. One of them is a stable 71-periodic cycle generated by

$$S^{71} \approx \left\{ \begin{pmatrix} 1.8598 \\ 0.76013 \\ 6.2305 \cdot 10^{-3} \end{pmatrix}, \dots \right\} .$$

Additionally, we find a second stable cycle which is 142-periodic,

$$S^{142} \approx \left\{ \begin{pmatrix} 1.93364 \\ 0.60068 \\ 0.20656 \cdot 10^{-3} \end{pmatrix}, \dots \right\} .$$

We computed the eigenvalues of these cycles,

$$|e_{1,2}(S^{71})| \approx |0.6477 \pm 0.3656i| \qquad = 0.7438 < 1, e_3(S^{71}) \approx 0, \tag{14}$$

$$|e_{1,2}(S^{142})| \approx |0.5079 \pm 0.3626i| \qquad = 0.6241 < 1, e_3(S^{142}) \approx 0. \tag{15}$$

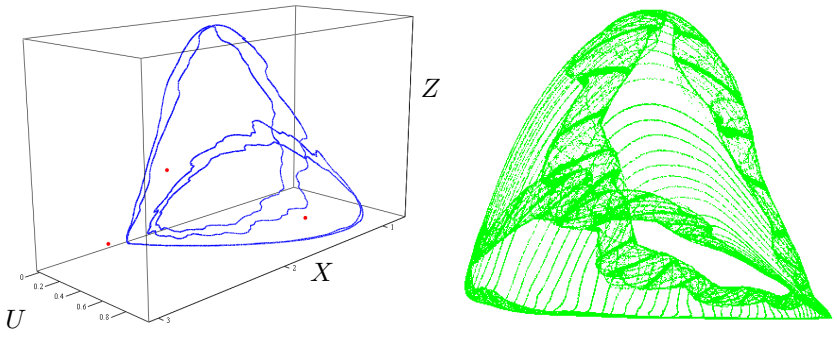

(a) (b)

Figure 9: *(a) Numerical approximation of the minimal attractor* $\mathcal{A}$ *at* $M_0 = 3.5501$ *(blue), which is a quasi-periodic cycle, and the fixed points (red). (b) Numerical approximation of* $\mathcal{M}$ *and* $\mathcal{M}_2$ *by curve iterates at* $M_0 = 3.56$.

All eigenvalues are < 1, and so we can verify the stability of these cycles. Obviously, both cycles are minimal coexisting attractors of the system. They are illustrated in Fig. 10.

Additionally, by use of the RIM method, 2 unstable periodic cycles can be found. One of them is 71-periodic,

$$U^{71} \approx \left\{ \begin{pmatrix} 1.02136 \\ 0.36569 \\ 0.4285 \end{pmatrix}, \dots \right\} ,$$

and the other one is 142-periodic,

$$U^{142} \approx \left\{ \begin{pmatrix} 1.7406 \\ 0.10355 \\ 1.3340 \end{pmatrix}, \dots \right\} .$$

Again, we analyze the eigenvalues of these cycles, which can be approximated as

$$e_1(U^{71}) \approx 1.4817, \qquad e_2(U^{71}) \approx 0.5603, \qquad e_3(U^{71}) \approx 0 \tag{16}$$

$$e_1(U^{142}) \approx 1.8779, \qquad e_2(U^{142}) \approx -0.0669, \qquad e_3(U^{142}) \approx 0 \tag{17}$$

The periodic cycles U^{71} and U^{142} are of saddle type. Their unstable manifolds are 1-dimensional. A numerical approximation is illustrated in Figs. 11 and 12. As can be seen, the visualization of the unstable manifolds significantly contributes to the understanding of the dynamics. It becomes obvious that there is a two-dimensional invariant manifold which contains all periodic cycles and is non-orientable. Geometrically, the manifold winds around a Möbius strip.

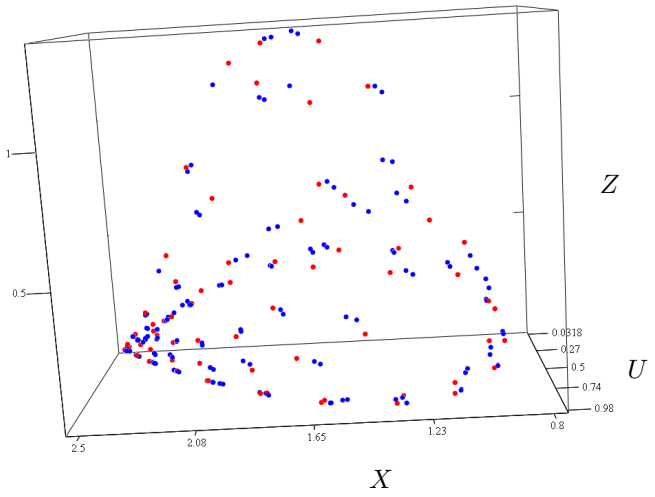

Figure 10: *The two co-existing attractors* S_1^{71} *(red) and* S^{142} *(blue) at* $M_0 = 3.571$.

The unstable manifold of U^{142} ends in S^{142} and S^{71}, whereby it seems that the unstable manifolds of U^{142} and U^{71} meet each other close to S^{71}. One half of the unstable manifold of U^{71} ends in S^{71}, and the other points towards U_2^{71}. We do not give here a more detailed discussion about the properties of the stable and unstable manifolds. Reason for this is that indeed the transition to chaos can be observed at this position in parameter space. A more detailed discussion is out of scope for this paper.

We point out that the maximum number of coexisting attractors is at least three in our biological system and end up with an investigation of the system at $M_0 = 3.5708$. At this position, three coexisting attractors can be localized. These are two cycles of period 71 denoted by $S_{1,2}^{71}$ and one cycle of period 142 denoted by S_1^{142}. The attractors can be generated by

$$S_1^{71} \approx \left\{ \begin{pmatrix} 1.0898 \\ 0.3074 \\ 0.3518 \end{pmatrix}, \ldots \right\} \ , \ S_2^{71} \approx \left\{ \begin{pmatrix} 1.0646 \\ 0.3259 \\ 0.3185 \end{pmatrix}, \ldots \right\}$$

and

$$S^{142} \approx \left\{ \begin{pmatrix} 1.0919 \\ 0.3065 \\ 0.3500 \end{pmatrix}, \ldots \right\} .$$

The attractors are illustrated in Fig. 13. Indeed, we guess that a still higher number of coexisting attractors exist in the interval $M_0 \in [3.5708; 3.571]$.

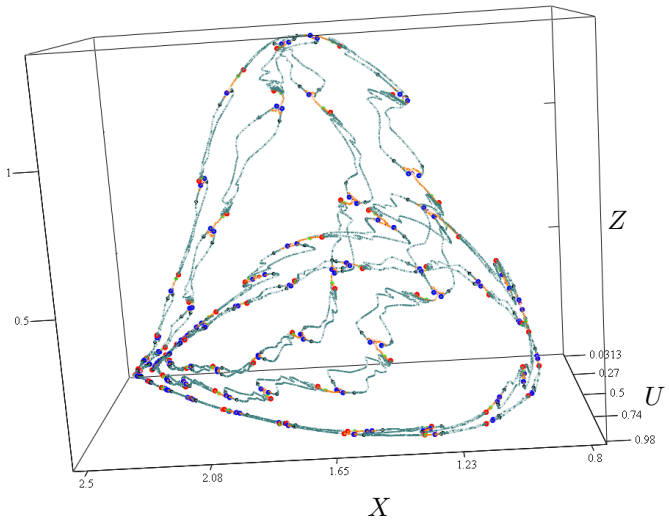

(a)

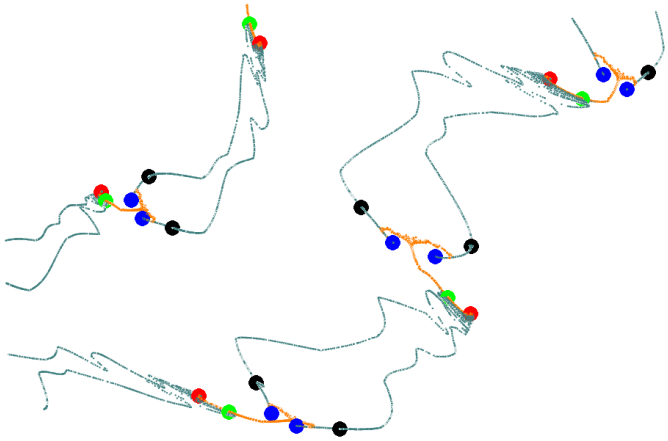

(b)

Figure 11: *(a)+(b): The two co-existing attractors S^{71} (red) and S^{142} (blue) at $M_0 = 3.571$ and an approximation of the saddles U^{71} (green) and U^{142} (black) and their unstable manifolds $W^s(U^{71})$ (orange) and $W^s(U^{142})$ (grey).*

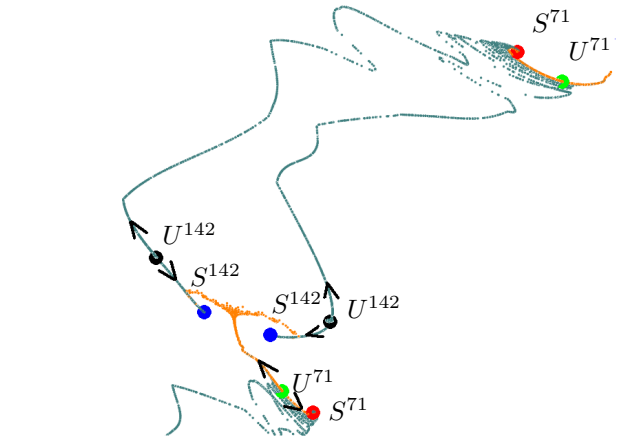

Figure 12: *Parts of the two co-existing attractors S^{71} (red) and S^{142} (blue) and of the unstable manifolds of the saddles U^{71} (orange) and U^{142} (grey). Arrows indicate the direction of the flow.*

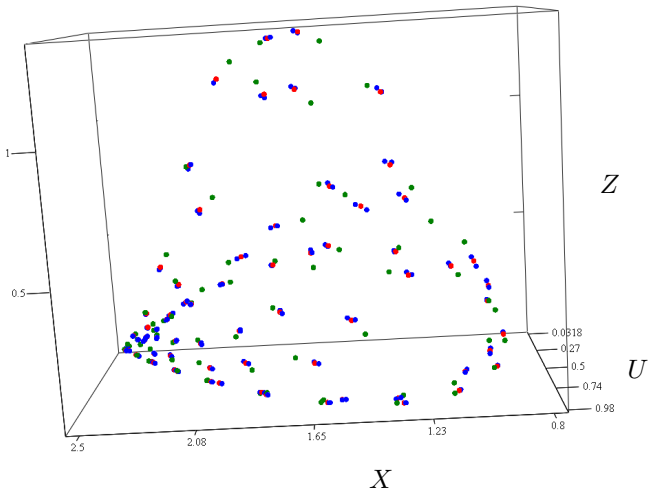

Figure 13: *The three co-existing attractors S_1^{71} (red), S_2^{71} (green) and S^{142} (blue) at $M_0 = 3.5708$.*

6 Conclusion

In this paper we have proved that a real discrete system with biological origin possesses a non-orientable invariant manifold, i.e. a Möbius strip. We also indicated that multiple attractors may arise in the system and estimated parts of the domains of attraction for some of these attractors.

The obtained results concerning multiple attractors in food-chains is that we have found several parameter regions possessing such phenomena and that we have been able to locate at least one region possessing at least three coexisting attractors. The cases so far detected possess attractors that are located close to each other in phase space. However, we have not been able to exclude more complicated situations having more intriguing biological consequences in the system under study or nearby systems, either.

General questions of biological importance are those related to persistence of species (Butler and Waltman (1986), Waltman (1992) and Rosenzweig (1971)) and regular or irregular population outbreaks (Elton (1930), Hanski, Hansson, and Henttonen (1991), and Andreasen (2003)) with respect to environmental parameters that describe the surrounding environment. The notion of persistence is related to food-chain length (May (1971)) and gives valuable insight on what kind of species are going to invade (as consequences of evolution) and or become eradicated in the ecology under study. Recently, the notion of persistence have been better understood in simple cases by extended understanding of the stochastic processes involved (Nåsell (2001)).

In this paper we call into question the status of the environmental parameters as a sole indicator of how an ecology evolves. Indeed, we argue that multiple attractors are a rather general phenomenon in larger ecological communities. This implies that the long-run behavior of the system might be sensitive to disturbances like temporary harvesting not involving permanent changes in the environmental parameters themselves. Our results do not imply that the detected changes were remarkable or catastrophic, but they are not more to be excluded. This also gives rise to intriguing problems when analyzing properties of ecological time-series (Royama (1992), Stenseth, Bjørnstad, and Falck (1996), and Ellner and Turchin (1995)). Our work leaves also a significant contribution to the understanding of the geometry of the invariant sets in typical food-chain systems. Orientability of these sets can not more be taken for granted, and non-orientability is a rather general property of these sets.

Acknowledgements The research of T. Lindström was financed by the Swedish Research Council. The research of G. Osipenko was financed by the Royal Swedish Academy of Sciences. T. Lindström and G. Osipenko thank the Royal Swedish Academy of Sciences for generous support in form of travel grants.

References

[1] Home page of the AnT 4.669 project, 2005. Available at `http://www.AnT4669.de`.

[2] V. Andreasen. Dynamics of annual influenza a epidemics with immuno selection. *Journal of Mathematical Biology*, 46:504–536, 2003.

[3] D. G. Aronson, M. A. Chory, G. R. Hall, and R. P. McGehee. Bifurcations from an invariant circle for two-parameter families of maps of the plane: A computer-assisted study. *Communications in Mathematical Physics*, 83:303–354, 1982.

[4] V. Avrutin, D. Fundinger, P. Levi, G. S. Osipenko, and M. Schanz. Investigation of dynamical systems using symbolic images: Efficient implementation and applications. Accepted for publication by International Journal of Bifurcation and Chaos, 2006.

[5] V. Avrutin, R. Lammert, M. Schanz, G. Wackenhut, and G. S. Osipenko. On the software package AnT 4.669 for the investigation of dynamical systems. In G. S. Osipenko, editor, *Fourth International Conference on Tools for Mathematical Modelling*, volume 9, pages 24 – 35. St. Petersburg State Polytechnic University, Russia, June 2003.

[6] G. Butler and P. Waltman. Persistence in dynamical systems. *Journal of Differential Equations*, 63:255–263, 1986.

[7] R. Devaney. *An Introduction to Chaotic Dynamical Systems*. Addison-Wesley Publishing Company, Inc, 1989.

[8] S. Ellner and P. Turchin. Chaos in a noisy world: New methods and evidence from time-series analysis. *The American Naturalist*, 145(3):343–375, 1995.

[9] C. Elton. *Animal ecology and evolution*. Clarendon Press, 1930.

[10] M. J. Feigenbaum. Quantitative universality for a class of nonlinear transformations. *J. Stat. Phys.*, 19:25 – 52, 1978.

[11] M. J. Feigenbaum. Universal behavior in nonlinear systems. *Los Alamos Sci.*, 1:4 – 27, 1980.

[12] D. Fundinger. Investigating dynamics by symbolic analysis: Tunings for an efficient computation of the symbolic image. *Differential Equations and Control Processes*, (3):16–37, 2005.

[13] D. Fundinger. *Investigation Dynamics by Multilevel Phase Space Discretization*. PhD thesis, University of Stuttgart, 2006.

[14] A. Gragnani, O. De Feo, and S. Rinaldi. Food chains in the chemostat: Relationships between mean yield and complex dynamics. *Bulletin of Mathematical Biology*, 60:703–719, 1998.

[15] J. Guckenheimer and P. Holmes. *Nonlinear Oscillations, Dynamical Systems, and Bifurcations of Vector Fields*. Springer-Verlag, 1983.

[16] M. Gyllenberg, I. Hanski, and T. Lindström. A predator-prey model with optimal suppression of reproduction in the prey. *Mathematical Biosciences*, 134:119–152, 1996.

[17] I. Hanski, L. Hansson, and H. Henttonen. Specialist predators, generalist predators, and the microtine rodent cycle. *Journal of Animal Ecology*, 60:353–367, 1991.

[18] A. Klebanoff and A. Hastings. Chaos in three species food chains. *Journal of Mathematical Biology*, 32:427–451, 1994.

[19] Y. A. Kuznetsov. *Elements of Applied bifurcation theory*. Springer, New York, 1998.

[20] Y. A. Kuznetsov, O. De Feo, and S. Rinaldi. Belyakov homoclinic bifurcations in a tritrophic food chain model. *SIAM Journal of Applied Mathematics*, 62(2):462–487, 2001.

[21] T. Lindström. On the dynamics of discrete food-chains: Low- and high-frequency behavior and chaos. *Journal of Mathematical Biology*, 45:396–418, 2002.

[22] R. M. May. Stability in multispecies community models. *Mathematical Biosciences*, 12:59–79, 1971.

[23] I. Nåsell. Extinction and quasi-statinarity in the Verhulst logistic model. *Journal of Theoretical Biology*, 211(1):11–27, 2001.

[24] G. S. Osipenko. On a symbolic image of dynamical system. *Interuniv. Collect. sci. Works*, pages 101 – 105, 1983. In Russian.

[25] G. S. Osipenko. *Lectures on symbolic analysis of dynamical systems*. St. Petersburg State Polytechnic University, 2004.

[26] M. L. Rosenzweig. Paradox of enrichment: Destabilization of exploitation ecosystems in ecological time. *Science*, 171:385–387, 1971.

[27] M. L. Rosenzweig. Exploitation in three throphic levels. *The American Naturalist*, 107(954):275–294, 1973.

[28] T. Royama. *Analytical Population Dynamics*. Chapman & Hall, 1992.

[29] N. C. Stenseth, O. N. Bjørnstad, and W. Falck. Is spacing behaviour coupled with predation causing the microtine density cycle? A synthesis of current process-oriented and pattern-oriented studies. *Proceedings of the Royal Society of London B*, 263:1423–1435, 1996.

[30] P. Waltman. A brief survey of persistence in dynamical systems. *Springer Lecture notes in Mathematics*, 1475:31–40, 1992.

[31] S. Wiggins. *Introduction to applied nonlinear dynamical systems and chaos.* Springer, New York, 2003.

[32] A. Wolf, J. B. Swift, H. L. Swinney, and J. A. Vastano. Determining Lyapunov exponents from a time series. *Physica D*, 16:285 – 317, 1985.